

國立交通大學

電子工程學系

碩士論文

用於多輸入多輸出通道的球體解碼演算法



A Sphere Decoding Algorithm for MIMO Channels

研究生：洪晉運

指導教授：桑梓賢 教授

中華民國九十五年六月


用於多輸入多輸出通道的球體解碼演算法

研究生： 洪晉運 指導教授： 桑梓賢 博士

國立交通大學

電子工程學系 電子研究所碩士班

摘要



多輸入多輸出 (MIMO) 傳輸已經是一種用來增加頻寬效益的眾所周知的技術。同時，如何設計出在多輸入多輸出通道使用的低運算量的接收器仍然是一項艱難的挑戰。最大概似偵測器 (ML detector) 可以達到極好的效能，然而其所需的計算量是非常龐大的。使用球體解碼演算法 (Sphere Decoding Algorithm) 可以達到和最大概似偵測器一樣的效能，並且可以降低大量的運算量。在此篇論文中，我們提出了一種較實用的球體解碼演算法。利用了一種簡單而且有效率的方法來設定球體的半徑初值，其扮演著決定計算量的一個很重要的角色。此外，我們利用一種增加虛擬天線的架構使得球體演算法能被應用在當傳送天線個數大於接收天線個數的情況；這個方法增加了球體解碼演算法更大的可用性，而且不致改變它原有的低運算量及高效能的特性。

A Sphere Decoding Algorithm for MIMO Channels

研 究 生：洪晉運

student : *Chin-Yun Hung*

指 導 教 授：桑梓賢

Advisors : *Tzu-Hsien Sang*

Department of Electronics Engineering & Institute of Electronics
National Chiao Tung University

ABSTRACT

Multi-Input Multi-Output (MIMO) transmission has become a popular technique to increase spectral efficiency. Meanwhile, the design of cost-effective receivers for MIMO channels remains a challenging task. Maximum-Likelihood (ML) detector can achieve superb performance, yet the computational complexity is enormously high. Receivers based on sphere decoding (SD) reach the performance of ML detectors, and potentially a great deal of computational cost can be saved. In this thesis, a practical sphere-decoding algorithm is proposed. It utilizes a simple and effective way to set the initial radius which plays a decisive role in determining the computational complexity. Furthermore, a pseudo-antenna augmentation scheme is employed such that sphere decoding can be applied where the number of receive antennas is less than that of transmit antenna; thus enhance the applicability of this powerful algorithm.

誌 謝

這篇論文能夠順利完成，首先要感謝指導教授 桑梓賢博士。當我在研究遇到瓶頸和挫折時，謝謝老師耐心的指引與教導，使我能及早確定研究方向，事半功倍。而最重要的要感謝我的父親 洪明鎮先生與母親 洪羅素珍女士這麼多年來的養育栽培之恩，無論我做什麼決定總是願意支持我。另外我要感謝啟仁學長，欣德學長，以及其他學長及同學，在我遇到問題時，總是不厭其煩的教導我，也給了我很多的建議和鼓勵，讓我在研究所期間過得更順利也更充實。最後還有謝謝我的女朋友—小嫻，謝謝妳一路陪著我考上研究所還有研究所期間，在我低潮時、壓力大的時候，始終陪在我身旁，默默忍受著我的脾氣，支持我，讓我很快樂的度過這幾年。謝謝！



Contents

| | |
|--|-----|
| 中文摘要..... | I |
| ABSTRACT..... | II |
| 誌謝..... | III |
| ACKNOWLEDGE | |
| CONTENTS..... | IV |
| LIST OF TABLES..... | VI |
| LIST OF FIGURES..... | VI |
| SYMBOLS..... | VII |
| | |
| Chapter 1 | 1 |
| Introduction | 1 |
| 1.1 Introduction | 1 |
| 1.2 Thesis Outline..... | 1 |
| | |
| Chapter 2 | 2 |
| Multiple-Input Multiple-Output | 2 |
| 2.1 MIMO System Model | 2 |
| 2.2 MIMO Receivers..... | 3 |
| 2.2.1 Linear Detection Methods..... | 3 |
| 2.2.2 Nulling and Cancelling..... | 3 |
| 2.2.3 Brute-Force Maximum Likelihood (ML) Detection..... | 4 |
| 2.2.4 Sphere Decoding (SD) | 5 |
| | |
| Chapter 3 | 8 |
| Sphere Decoding Algorithm..... | 8 |
| | |
| Chapter 4 | 11 |
| The Proposed Sphere Decoding Algorithm | 11 |
| 4.1 Setting the Radius..... | 11 |
| 4.2 A Pseudo-Antenna Augmentation Scheme | 13 |
| | |
| Chapter 5 | 20 |
| Simulation Results..... | 20 |

| | |
|-------------------|----|
| Chapter 6 | 23 |
| Conclusion..... | 23 |
| Future work | 24 |
| Appendix | 29 |
| Reference..... | 31 |



LIST OF TABLES

| | |
|---|----|
| Table I. Summary of comparative performance of receivers for spatial multiplexing. | 7 |
| Table II. The probability of minimum column norm equal to minimum decision distance. | 22 |

LIST OF FIGURES

| | |
|--|----|
| Figure 2.1 MIMO system block diagram..... | 3 |
| Figure 2.2 Concept behind the sphere decoder. | 6 |
| Figure 3.1 Sample tree generated to determine lattice points in a $N_T = 3$ hypersphere. | 10 |
| Figure 4.1 The diagram shows the idea of finding a proper radius. Assume BPSK and a 2×2 channel matrix for simplicity. | 13 |
| Figure 4.2 The diagram of an augmented 2×2 MIMO system. | 16 |
| Figure 4.3(a) The space diagram of the transmitted symbol vectors..... | 16 |
| Figure 4.3(b) The pseudo received signal vectors. Assume $N_T = 2$, $N_R = 1$, BPSK modulation and $h_1 > h_2 > 0$ for simplicity. Define $b_1 = h_1 + h_2$, $b_2 = h_1 - h_2$, $b_3 = -h_1 + h_2$, and $b_4 = -h_1 - h_2$ for convenience..... | 16 |
| Figure 4.3(c) The augmented received signal vectors. | 17 |
| Figure 4.4 The space diagram of the hypersphere D when a is very large. Assume BPSK and a 2×1 MIMO channel for simplicity. | 18 |
| Figure 5.1 The BER curves of SD and brute-force ML detector. Assume $N_T = 6$, $N_R = 3$, QPSK, spatial multiplexing, and $a = 0.1 + 0.1j$ | 20 |
| Figure 5.2 The average number of candidates inside sphere D with different values of a and $\frac{E_b}{N_0}$. Assume $N_T = 6$, $N_R = 3$ and QPSK modulation. | 21 |
| Figure 6.1 The flowchart of decoding algorithm | 28 |

Symbols

| | |
|----------------------------|--|
| N_T | : The number of transmit antennas |
| N_R | : The number of receive antennas |
| $(\bullet)^H$ | : Hermitian transpose operation |
| $\mathcal{R}^{m \times n}$ | : m-by-n real valued matrix |
| $\mathcal{C}^{m \times n}$ | : m-by-n complex valued matrix |
| \mathcal{R}^m | : m-by-1 real valued vector |
| \mathcal{C}^m | : m-by-1 complex valued vector |
| $R\{\bullet\}$ | : Real part operation |
| $I\{\bullet\}$ | : Image part operation |
| $E\{\bullet\}$ | : Expectation value operation |
| $\min_i a_i$ | : Minimum of a_i |
| $(\mathbf{A})_i$ | : The i-th column of matrix \mathbf{A} |

Chapter 1

Introduction

1.1 Introduction

Sphere Decoding has recently been applied to signal detection problem for Multi-Input Multi-Output (MIMO) systems [1]–[4]. It is a reduced search algorithm for doing ML detection. Notice that brute-force ML detection has computational complexity that is exponentially growing in the number of sub-streams, the constellation size, and the number of transmit antennas; as a result, it is not feasible for practical systems. Indeed, SD holds the potential of significantly reducing the computational cost while maintaining the superb performance of an ML detector and therefore is compared favorably with other sub-optimal detectors proposed for MIMO systems.

1.2 Thesis Outline

This thesis is organized as follows. The MIMO system model and some detection algorithms for MIMO system are laid out in Chapter 2. The basic sphere decoding algorithm is discussed in Chapter 3. The radius-setting method and the pseudo-antenna augmentation scheme are described in Chapter 4. Simulation results are presented in Chapter 5, and finally, a brief conclusion in Chapter 6.

Chapter 2

Multiple-Input Multiple-Output

2.1 MIMO System Model

For getting high data rates on a rich-scattering wireless channel without increasing transmit power, a technique is to use multiple transmit and receive antennas, the so called multiple-input multiple-output (MIMO) system. MIMO technique uses spatial diversity to fight multipath fading in wireless channels and also enhance channel capacity.

The MIMO system model is as follow. Assume N_T transmit antennas and N_R receive antennas. Let \mathbf{s} be the transmitted vector symbols (also referred to as “vector constellation symbol”) in \mathcal{R}^{N_T} or \mathcal{C}^{N_T} whose entries are chosen from some complex constellation \mathcal{O} (e.g. QPSK, 16-QAM etc.). The received signal is given by

$$\mathbf{y} = \mathbf{H}\mathbf{s} + \mathbf{n} \quad (1.1)$$

where $\mathbf{y} \in \mathcal{C}^{N_R}$ is the received signal vector, $\mathbf{H} \in \mathcal{C}^{N_R \times N_T}$ is the Rayleigh flat fading channel matrix, and the entries of \mathbf{n} is the additive i.i.d. zero mean circularly symmetric complex Gaussian (ZMCSCG) noise with variance of σ^2 , i.e., $n_k \sim CN(0, \sigma^2)$, $k = 1, \dots, N_R$.

Figure 2.1 shows the block diagram of a simple MIMO system.

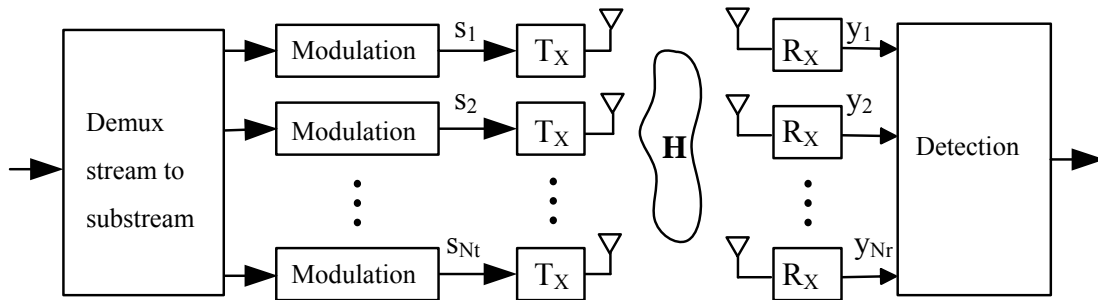


Figure 2.1 MIMO system block diagram.

2.2 MIMO Receivers

Some detection algorithms for MIMO systems are reviewed in the following.



2.2.1 Linear Detection Methods

The linear detection method first estimates the channel matrix then tries to compensate (inverse) the channel effect by another matrix. The inverse matrix is usually based on Zero Forcing (ZF) or Minimum Mean Square Error (MMSE) criterion. This method requires very low computational complexity, but results in significant performance degradation.

2.2.2 Nulling and Cancelling

Successive interference cancellation (SIC) peels the transmission signal

apart one data stream at a time. It decodes and cancels the data stream iteratively until all transmitted streams are resolved. If sorting is done to determine the decoding order from the highest to the lowest SNR, it is called ordered successive interference cancellation (OSIC). An example is the so-called Vertical Bell-laboratory LAYered Space-Time (V-BLAST) receiver [5]. OSIC has a slightly better performance than SIC does, but is still suboptimal and suffers from error propagation.

2.2.3 Brute-Force Maximum Likelihood (ML) Detection

Assuming that the transmitted data sequence is i.i.d., the maximum likelihood detector for a MIMO system performs the operation:

$$\begin{aligned}\hat{\mathbf{s}}_{ML} &= \arg \min_{s \in \mathcal{O}^{N_T}} \|\mathbf{y} - \mathbf{H}\mathbf{s}\|^2 \\ &= \arg \min_{s \in \mathcal{O}^{N_T}} (\mathbf{y} - \mathbf{H}\mathbf{s})^H (\mathbf{y} - \mathbf{H}\mathbf{s})\end{aligned}\quad (1)$$

where \mathbf{y} is the observed vector signal, \mathbf{H} is the channel matrix whose size is $N_R \times N_T$, \mathcal{O}^{N_T} is the entire set of possible transmitted vector symbols, \mathcal{O} is the complex-valued modulating constellation, and $(\cdot)^H$ means Hermitian transpose. The ML detector is optimal in terms of symbol error rate, but the computational complexity can be prohibitively high if it is implemented by exhaustively searching over \mathcal{O}^{N_T} .

2.2.4 Sphere Decoding (SD)

In 1985, U. Fincke and M. Phost proposed an algorithm named Fincke-Phost algorithm [6] (or SD algorithm) which offers a large reduction in computational complexity for the class of computationally-hard combinatorial problems, for instance, the aforementioned ML detection problem. SD algorithm used for resolving MIMO channel was presented in [1]–[4] and was shown to reduce the complexity of ML detector significantly [1], [7], [8]. The enormous computational complexity of ML detector arises from the huge number of vector symbols to be compared in order to find the solution in (1). The main idea of SD algorithm is to use a highly efficient method to reduce the number of candidate vector symbols before the actual comparison happens. For more on the efficiency of SD, please refer to [1], [7], [8].

Let \mathcal{D} be a sphere centered at the received vector \mathbf{y} , and the radius d of \mathcal{D} is properly defined such that only a small number of vector symbols fall inside \mathcal{D} after being transformed by the channel matrix. The search of the closest transformed vector symbol to \mathbf{y} can be conducted among these candidates in \mathcal{D} rather than the entire set \mathcal{O}^{N_T} , thereby reducing the search space and hence the required computations. Figure 2.2 shows a space diagram of the concept of sphere decoding algorithm. A well-designed sphere decoder would have performance equal to that of an ML detector. For example, it can reach full diversity while V-BLAST can only reach $N_R \times N_T + 1$ [9].

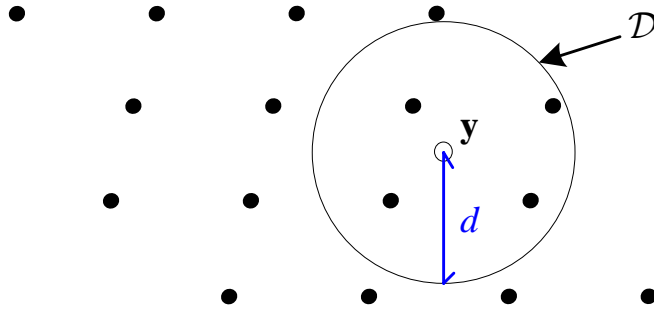


Figure 2.2 Concept behind the sphere decoder.

Two questions need to be addressed for an effective sphere decoder to be constructed:

1. How to choose the radius d such that the number of candidates is well limited?
2. How to determine efficiently if a channel symbol actually lies inside the hypersphere \mathcal{D} ?

In this paper, a simple yet effective method to set the radius of the hypersphere \mathcal{D} is proposed. A pseudo-antenna augmentation scheme is also proposed such that SD can efficiently determine the position of a lattice point relative to \mathcal{D} in the case where the number of transmit antennas is larger than the number of receive antennas, thus expand the applicability of SD. Compared to existing literatures which handle rank deficient channel matrices [2], [10]–[12], our method is more intuitive and straightforward, and it enjoys a computational complexity in polynomial when SNR is sufficiently high, while methods in [2], [10], [11] have a complexity growing exponentially in $(N_T - N_R)$.

The comparison of diversity order and SNR loss of some detection methods

of MIMO system with spatial multiplexing are presented in Table I. [9].

| Receiver | Diversity order | SNR loss |
|----------|--------------------------------|----------|
| ZF | $N_R - N_T + 1$ | High |
| MMSE | $\cong N_R - N_T + 1$ | Low |
| SIC | $\cong N_R - N_T + 1$ | Low |
| OSIC | $\geq N_R - N_T + 1, \leq N_R$ | Low |
| ML | N_R | Zero |

Table I. Summary of comparative performance of receivers for spatial multiplexing.



Chapter 3

Sphere Decoding Algorithm

Herein we will discuss the details of basic sphere decoding algorithm. Assume $N_R \geq N_T$, and channel matrix \mathbf{H} is column independent and real value, \mathbf{H} can be QR-factorized [13] as

$$\begin{aligned} \mathbf{H} &= \mathbf{Q}\mathbf{R} \\ &= [\mathbf{Q}_1 \quad \mathbf{Q}_2] \begin{bmatrix} \mathbf{R}' \\ \mathbf{0} \end{bmatrix} \end{aligned} \quad (3.1)$$

where $\mathbf{Q} \in \mathcal{R}^{N_R \times N_R}$ is an orthonormal matrix, $\mathbf{R} \in \mathcal{R}^{N_R \times N_T}$ is an upper triangular matrix, and \mathbf{R}' is an $N_T \times N_T$ upper triangular matrix of \mathbf{R} . The matrices \mathbf{Q}_1 and \mathbf{Q}_2 consist of the first N_T and last N_T orthonormal columns of \mathbf{Q} respectively.

The lattice point $\mathbf{H}\mathbf{s}$ lies inside the hypersphere \mathcal{D} of radius d if and only if

$$d^2 \geq \|\mathbf{y} - \mathbf{H}\mathbf{s}\|^2. \quad (3.2)$$

From (3.1) and (3.2), we have

$$d^2 - \|\mathbf{Q}_2^H \mathbf{y}\|^2 \geq \|\mathbf{Q}_1^H \mathbf{y} - \mathbf{R}\mathbf{s}\|^2. \quad (3.3)$$

Define $d'^2 = d^2 - \|\mathbf{Q}_2^H \mathbf{y}\|^2$ and $\mathbf{z} = \mathbf{Q}_1^H \mathbf{y}$, and (3.3) becomes

$$d'^2 \geq \sum_{i=1}^{N_T} \left(z_i - \sum_{j=i}^{N_T} r_{ij} s_j \right)^2. \quad (3.4)$$

The RHS of (2.4) can be expanded as

$$\left(z_{N_T} - r_{N_T, N_T} s_{N_T}\right)^2 + \left(z_{N_T-1} - r_{N_T-1, N_T} s_{N_T} - r_{N_T-1, N_T-1} s_{N_T-1}\right)^2 + \dots \quad (3.5)$$

where the first term depends only on s_{N_T} , the second term depends on both s_{N_T} and s_{N_T-1} and so on. Hence one necessary condition for $\mathbf{H}\mathbf{s}$ lies inside the hypersphere \mathcal{D} is $d'^2 \geq \left(z_{N_T} - r_{N_T, N_T} s_{N_T}\right)^2$. This condition leads to s_{N_T} belonging to the interval

$$\left[\frac{-d' + z_{N_T}}{r_{N_T, N_T}} \right] \leq s_{N_T} \leq \left[\frac{d' + z_{N_T}}{r_{N_T, N_T}} \right]. \quad (3.6)$$

For every s_{N_T} satisfying (3.6), defining $d_{N_T-1}'^2 = d_{N_T}'^2 - \left(z_{N_T} - r_{N_T, N_T} s_{N_T}\right)^2$ and $z_{N_T-1|N_T} = z_{N_T-1} - r_{N_T-1, N_T} s_{N_T}$, a stronger necessary condition can be found as

$$d_{N_T-1}'^2 \geq \left(z_{N_T-1|N_T} - r_{N_T-1, N_T-1} s_{N_T-1}\right)^2, \quad (3.7)$$

and that is equivalent to

$$\left[\frac{-d'_{N_T-1} + z_{N_T-1|N_T}}{r_{N_T-1, N_T-1}} \right] \leq s_{N_T-1} \leq \left[\frac{d'_{N_T-1} + z_{N_T-1|N_T}}{r_{N_T-1, N_T-1}} \right]. \quad (3.8)$$

We can also do this search method to find possible s_{N_T-2} related to s_{N_T} and s_{N_T-1} we found, and so on until possible s_1 found. Thereby we can obtain all candidates belonging to (3.2). Next, the set of all candidates is searched and the one closed to the received signal vector is chosen to generate the decoding result [1], [3], [9], [14].

If \mathbf{H} , \mathbf{y} , \mathbf{s} , and \mathbf{n} are complex-valued, they can be written as

$$\begin{aligned}
\mathcal{H} &= \begin{bmatrix} \text{R}\{\mathbf{H}\} & -\text{I}\{\mathbf{H}\} \\ \text{I}\{\mathbf{H}\} & \text{R}\{\mathbf{H}\} \end{bmatrix} \\
\mathcal{Y} &= \begin{bmatrix} \text{R}\{\mathbf{y}\} \\ \text{I}\{\mathbf{y}\} \end{bmatrix} \\
\mathcal{S} &= \begin{bmatrix} \text{R}\{\mathbf{s}\} \\ \text{I}\{\mathbf{s}\} \end{bmatrix}
\end{aligned} \tag{3.9}$$

Then we can use (3.9) in substitution for \mathbf{H} , \mathbf{y} , and \mathbf{s} in (3.1) and (3.2).

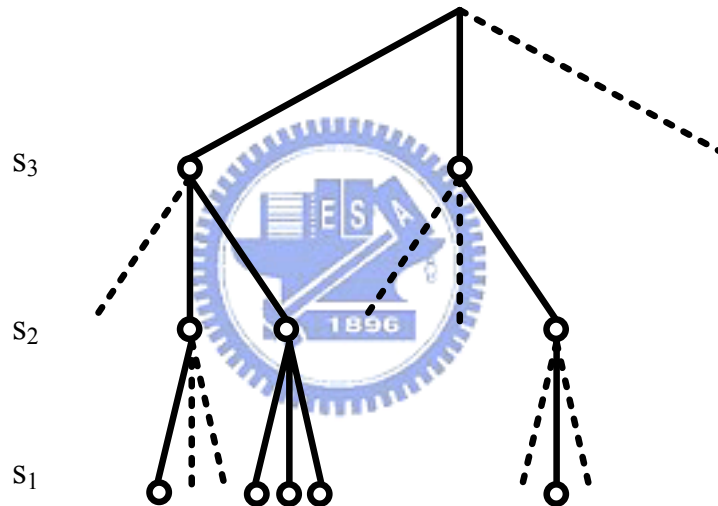


Figure 3.1 Sample tree generated to determine lattice points in a $N_T = 3$ hypersphere.

Fig. 3.1 shows the searching tree of the concept of sphere decoding algorithm. Assume $N_T = 3$, and s_i is takes on three possible values. The dotted lines are the points not satisfied (3.2), and circles are candidates.

Chapter 4

The Proposed Sphere Decoding Algorithm

To make the SD algorithm a practical choice for MIMO receiver design, two important modifications are proposed. The first is for finding a proper value for d and the second is a pseudo-antenna augmentation scheme to expand the applicable scope of SD. These modifications are discussed in the following two subsections.

4.1 Setting the Radius



In drawing the decision regions for an ML detector, the decision boundaries lie on the mid-lines between neighboring lattice points. If the shortest decision distance is used as the initial value of d , it is most likely that the SD algorithm finds one and only one candidate in the hypersphere \mathcal{D} when the noise is small enough that no decision errors occur (this is the case for most of the time). The shortest decision distance can be easily calculated for certain highly regular modulation constellations. For instance, the shortest decision distance in a square lattice is

$$\min_{i \neq j} \frac{1}{2} \|\mathbf{H}(\mathbf{s}_i - \mathbf{s}_j)\| \quad (4.1)$$

where \mathbf{s}_i and $\mathbf{s}_j \in \mathcal{O}^{N_T}$ are the transmitted symbol vectors. For square QAM, the minimum decision distance can be found as

$$\min_{k_i, l_i} \frac{1}{2} \left\| \sum_{i=1}^{N_T} [(-1)^{k_i} - (-1)^{l_i}] (\mathbf{H})_i \right\| \quad (4.2)$$

where $(\mathbf{H})_i$ denotes the i -th column of \mathbf{H} , k_i and l_i takes on the value 0 or 1, and the vector $[k_1, \dots, k_{N_T}] \neq [l_1, \dots, l_{N_T}]$. The expression of minimum distance can be further simplified as

$$\min_{k \in \{1, \dots, 3^{N_T} - 1\}} \left\| \sum_{i=1}^{N_T} c_{k_i} (\mathbf{H})_i \right\| \quad (4.3)$$

where $[c_{k_1}, \dots, c_{k_N_T}]$ represents all possible non-zero vectors whose elements take on values from $\{0, 1, -1\}$. Therefore, to find the minimum decision distance is to find the minimum norm over a set of random vectors with complex Gaussian elements.

To find the minimum norm in (4.3) is straightforward; nevertheless, it can take a long time if the problem dimension is large. Notice that among these random vectors, $(\mathbf{H})_1, \dots, (\mathbf{H})_{N_T}$ have the smallest expected norm. As a result, when N_T is large, the minimum norm will likely occur as the norm of some vector in $\{(\mathbf{H})_1, \dots, (\mathbf{H})_{N_T}\}$. Therefore, it is proposed that, instead of the minimum decision distance, the minimum column norm in (4.4) is used as the initial value of d . If no candidate point is found inside the hypersphere, then a larger value will be adopted and the SD procedure is repeated until a termination criterion is met. In short, we make

$$d_{initial} = \min_i \left\| (\mathbf{H})^i \right\| \quad (4.4)$$

where $i = 1, \dots, N_T$.

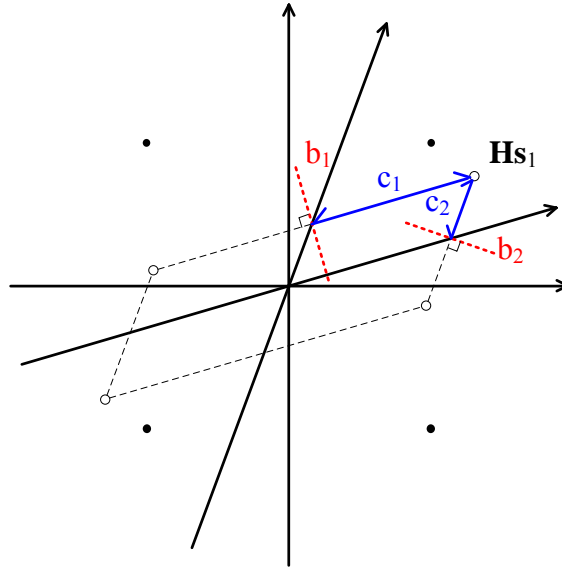


Figure 4.1 The diagram shows the idea of finding a proper radius. Assume BPSK and a 2×2 channel matrix for simplicity.

Fig. 4.1 shows the concept with a simple example of a 2×2 MIMO channel. Solid points represent the possible transmitted symbols, and circles are the received lattice points, i.e., the transmitted symbols multiplied by the channel matrix. Line b_1 and b_2 represent the mid-lines between neighboring points, and c_1 and c_2 are the two decision distances of $\mathbf{H}\mathbf{s}_1$. In this example, c_1 and c_2 are exactly the column norms of \mathbf{H} , and c_1 is chosen as the initial radius of hypersphere \mathcal{D} .

4.2 A Pseudo-Antenna Augmentation Scheme

Typical sphere decoders for MIMO channels can only handle the case where $N_R \geq N_T$ [1]. These sphere decoders fail when $N_T > N_R$ because \mathbf{H} does not have full column rank and therefore cannot be QR-factorized. Here, a

modification is proposed to deal with the case $N_T > N_R$.

The idea is to augment \mathbf{H} into a matrix with full column rank. Let the augmented matrix be

$$\tilde{\mathbf{H}}_{N_T \times N_T} = \begin{bmatrix} a & 0 & \cdots & \cdots & \cdots & \cdots & 0 \\ 0 & a & 0 & \cdots & \cdots & \cdots & 0 \\ \vdots & \ddots & \ddots & \ddots & \cdots & \cdots & \vdots \\ 0 & \cdots & 0 & a & 0 & \cdots & 0 \\ h_{11} & h_{12} & \cdots & \cdots & \cdots & \cdots & h_{1,N_T} \\ \vdots & \vdots & \cdots & \cdots & \cdots & \cdots & \vdots \\ h_{N_R,1} & h_{N_R,2} & \cdots & \cdots & \cdots & \cdots & h_{N_R,N_T} \end{bmatrix} \quad (4.5)$$

$$= \begin{bmatrix} a\mathbf{I}_{(N_T-N_R)} & \mathbf{0}_{(N_T-N_R) \times N_R} \\ \mathbf{H} & \end{bmatrix}$$

in which the bottom N_R rows comprise the original channel matrix, \mathbf{I} is the identity matrix, and a is either a small real or complex number depending on the modulation scheme. The pseudo received vector is defined as

$$\begin{bmatrix} as_1 \\ \vdots \\ as_{N_T-N_R} \\ \sum_{i=1}^{N_T} h_{1i}s_i + n_1 \\ \vdots \\ \sum_{i=1}^{N_T} h_{N_R,i}s_i + n_{N_R} \end{bmatrix}, \quad (4.6)$$

and the noise vector is augmented as

$$\begin{aligned}
\tilde{\mathbf{n}}_{N_T \times 1} &= \begin{bmatrix} -as_1 \\ \vdots \\ -as_{N_T-N_R} \\ n_1 \\ \vdots \\ n_{N_R} \end{bmatrix} \\
&= \begin{bmatrix} \mathbf{n}'_{(N_T-N_R) \times 1} \\ \mathbf{n}_{N_R \times 1} \end{bmatrix}
\end{aligned} \tag{4.7}$$

to make the final augmented received vector to be

$$\begin{aligned}
\tilde{\mathbf{y}}_{N_T \times 1} &= \begin{bmatrix} \mathbf{0}_{(N_T-N_R) \times 1} \\ \mathbf{y}_{N_R \times 1} \end{bmatrix} \\
&= \tilde{\mathbf{H}}\mathbf{s} + \tilde{\mathbf{n}}.
\end{aligned} \tag{4.8}$$

By this augmentation, $\tilde{\mathbf{H}}$ has full column rank and can be decomposed via standard QR factorization algorithms. The SD algorithm can now be applied with similar effectiveness for the case $N_T > N_R$. This method is similar but more straightforward than the method in [12] in which an augmented diagonal matrix $\alpha\mathbf{I}$ is added to the matrix $\mathbf{H}^H\mathbf{H}$ to make it full-rank. More comparisons will be made when the effect of a is analyzed.

The concept of pseudo-antenna augmentation is shown in Fig. 4.2 where a simple 2×1 MIMO channel is augmented to a 2×2 MIMO channel. Fig. 4.3(a) shows the space diagram of the transmitted symbol vector, fig. 4.3(b) shows the pseudo received signals space, and the augmented received signals space was shown in fig 4.3(c). From (3.6) and (3.8), the smaller the value of a is, the closer the augmented and pseudo received signals become. This observation

is also shown in Fig. 4.3(a)-(c).

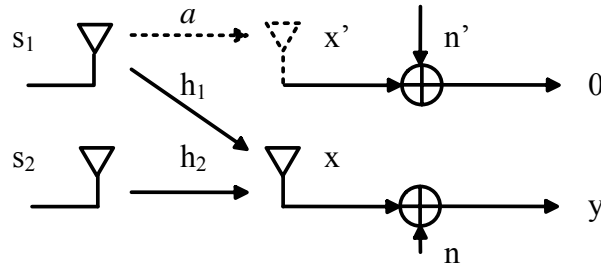


Figure 4.2 The diagram of an augmented 2×2 MIMO system.

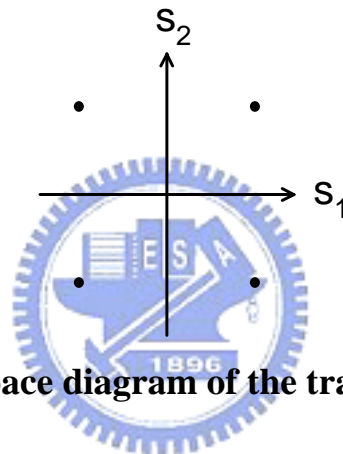


Figure 4.3(a) The space diagram of the transmitted symbol vectors.

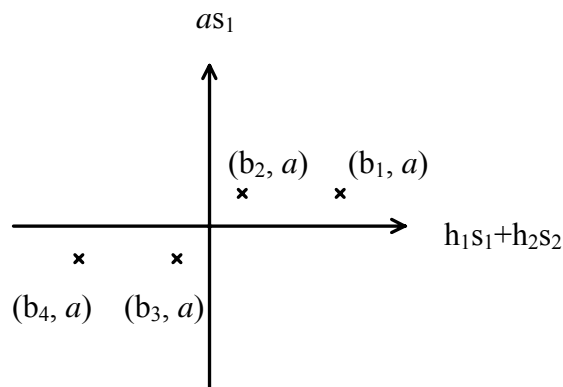


Figure 4.3(b) The pseudo received signal vectors. Assume $N_T = 2$, $N_R = 1$,

BPSK modulation and $h_1 > h_2 > 0$ for simplicity. Define $b_1 = h_1 + h_2$,

$b_2 = h_1 - h_2$, $b_3 = -h_1 + h_2$, and $b_4 = -h_1 - h_2$ for convenience.

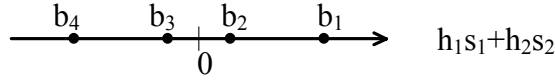


Figure 4.3(c) The augmented received signal vectors.

The effect of the value taken by a can be further analyzed as follows. The set of constellation points resulting in received signals inside the hypersphere \mathcal{D} is found as

$$s^{\mathcal{D}} = \left\{ \mathbf{x} \mid d^2 \geq \|\tilde{\mathbf{y}} - \tilde{\mathbf{H}}\mathbf{x}\|^2 \right\}. \quad (4.9)$$

The inequality in (3.9) can be expanded to

$$d^2 \geq |a|^2 \sum_{i=1}^{N_T-N_R} |s_i|^2 + \sum_{i=1}^{N_R} \left| \sum_{j=1}^{N_T} h_{ij} (s_j - x_j) + n_i \right|^2. \quad (4.10)$$

The lower bound of the radius d with which the correct symbol \mathbf{s} lies in the hypersphere, i.e., $\mathbf{x} = \mathbf{s} \in \mathbf{S}^{\mathcal{D}}$, depends on the noise condition and a . Assume QPSK for simplicity, then $|s_1|^2 = \dots = |s_{N_T-N_R}|^2 = 2$ and the lower bound in (3.10) satisfies

$$d_{LB}^2 \geq 2(N_T - N_R)|a|^2 + \sum_{i=1}^{N_R} |n_i|^2. \quad (4.11)$$

The expected lower bound is thus

$$E \left\{ d_{LB}^2 \right\} \geq 2(N_T - N_R)|a|^2 + N_R \sigma^2. \quad (4.12)$$

As can be seen clearly in (4.11), if a is small, the lower bound on the radius with which the correct symbol vector can be included is essentially independent of a . But if a is large, the radius needs to be large.

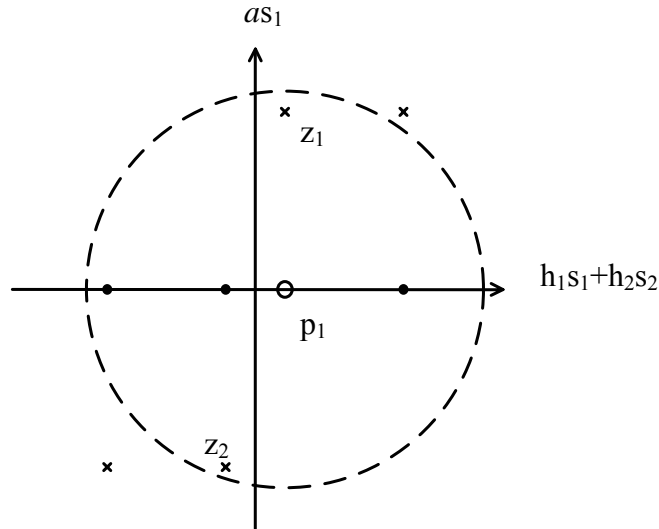


Figure 4.4 The space diagram of the hypersphere \mathcal{D} when a is very large.

Assume BPSK and a 2×1 MIMO channel for simplicity.

Fig. 4.4 shows the diagram of a simple example with a 2×1 MIMO channel, BPSK, and a large a . Let point p_1 be the augmented received signal and z_1 the pseudo received signal. The total number of possible received points is 4. As is said before, the radius of the sphere needs to be large. However, when setting the radius, it is extremely difficult for the decoder to find a radius barely large enough to include the lattice point corresponding to the correct symbol while avoid including wrong lattice points in the sphere simultaneously. In Fig. 4.4, the sphere not only contains the correct point z_1 but also z_2 . If a more sophisticated modulation such as 64-QAM is used, and the number of transmit antenna is larger, much more lattice points will inevitably be included in the large hypersphere, and the efficiency of SD will be greatly diminished. Therefore, a should be as small as possible, as long as the numerical stability is maintained in the computing process. With a small a , the complexity of SD is essentially independent of a and the same as that of usual SD algorithms, i.e.,

roughly $O(N_T^3)$ when SNR is high [1]. The efficiency of the method in [12], on the contrary, depends on the choice of α , and the optimal choice of α depends on noise condition and is not easy to find.

After the set of all candidate points is generated, the final step of the modified SD algorithm for MIMO channels works the same as the ML detector does. The estimated transmitted symbol vector $\hat{\mathbf{S}}$ is obtained by exhaustive search and equals to

$$\hat{\mathbf{s}} = \arg \min_{\mathbf{Hs} \in \mathcal{D}} \|\mathbf{y} - \mathbf{Hs}\|. \quad (4.13)$$



Chapter 5

Simulation Results

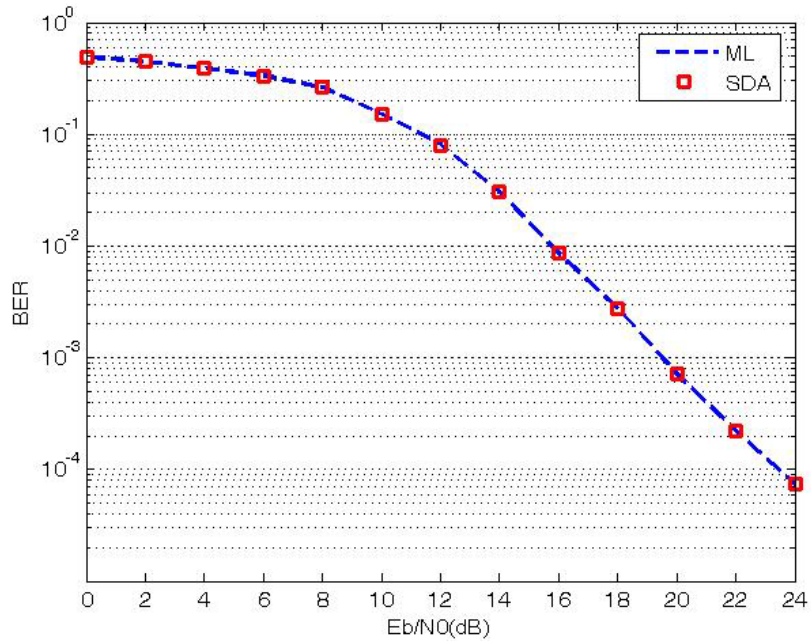


Figure 5.1 The BER curves of SD and brute-force ML detector. Assume $N_T=6$, $N_R=3$, QPSK, spatial multiplexing, and $a = 0.1 + 0.1j$.

Fig. 5.1 shows the performance of SD compared to that of ML receiver. The value of a is set to be very small and the BER performance is equal to that of a brute-force ML receiver.

Fig. 5.2 shows the average number of candidates found in \mathcal{D} when different values of a and $\frac{E_b}{N_0}$ and the proposed initial radius are used. Notice that when a is getting smaller, say, less than $0.1+0.1j$, the number of candidates found in \mathcal{D} is essentially independent of a and is only function of

SNR. Also notice that when SNR is moderately large, e.g., in the applications of spatial multiplexing, the number of candidates is close to 1. This means the proposed SD algorithm is operating in a very efficient manner.

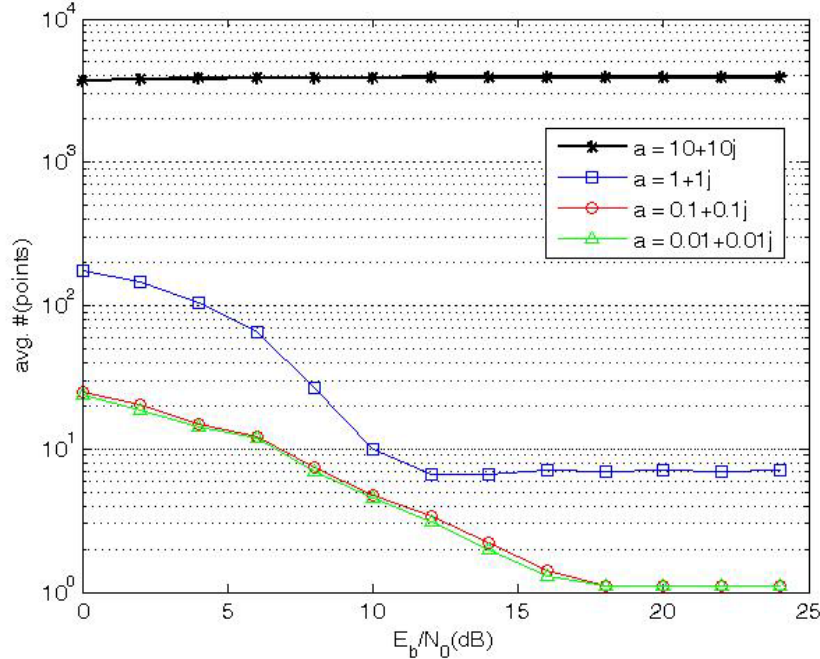


Figure 5.2 The average number of candidates inside sphere \mathcal{D} with different values of a and $\frac{E_b}{N_0}$. Assume $N_T = 6$, $N_R = 3$ and QPSK modulation.

Table II. lists the probabilities of when the minimum column norm coincides the minimum distance under different settings. For most of the time, when $N_T = N_R$, they do coincide. When $N_T > N_R$, the probability is not high. However, simulation (Fig. 5.2) shows that the minimum column norm is still an effective radius setter with moderate SNRs, judging from the low number of candidates found.

| | | N_T | | | |
|-------|----------|----------|----------|----------|----------|
| | | 2 | 4 | 6 | 8 |
| N_R | 2 | 0.8339 | 0.4537 | 0.1804 | 0.0553 |
| | 4 | 0.9327 | 0.7770 | 0.5650 | 0.3610 |
| | 6 | 0.9668 | 0.9010 | 0.7970 | 0.6650 |
| | 8 | 0.9859 | 0.9490 | 0.9170 | 0.8550 |

Table II. The probability of minimum column norm equal to minimum decision distance.



Chapter 6

Conclusion

SD algorithm can significantly lower the computational cost of ML detectors by reducing the number of possible candidates before executing the final step of exhaustive search. In this paper, two special features are introduced to enhance the capability of SD. First, a radius-setting method is used to keep the number of candidate lattice points consistently low. Second, a pseudo-antenna augmentation scheme is employed to cope with the situation where the number of transmit antennas is large than that of receive antennas, which happens often in real-world applications. In short, the modified SD algorithm constitutes an attractive option for practical MIMO receiver design.



Future work

Refer to [1], herein we will show a closed form of expected complexity of SD algorithm. From (1.1), $\frac{2}{\sigma^2} \|\mathbf{y} - \mathbf{H}\mathbf{s}\|^2 = \frac{2}{\sigma^2} \|\mathbf{n}\|^2$ is a χ^2 random variable with $\frac{n}{2}$ degrees of freedom where $n = 2N_R$ due to complex Gaussian noise vector. From (3.2), we may choose the radius d in such a way that with a high probability we find the transmitted vector inside the hypersphere \mathcal{D} as

$$\int_0^{d^2} \frac{\lambda^{\frac{n}{2}-1}}{\Gamma\left(\frac{n}{2}\right)} e^{-\lambda} d\lambda = 1 - \varepsilon, \quad (\text{A.1})$$

where $1 - \varepsilon$ is set to a value close to 1, say, $1 - \varepsilon = 0.99$. If the point is not found, we can increase the probability $1 - \varepsilon$, adjust the radius, and search again. Apply to the radius setting method in (4.4), if the radius in (A.1) is large than that in (4.4), we may enlarge the radius used in SD algorithm.

The complexity of SD algorithm is proportional to the number of nodes visited on the tree in searching tree as Fig. 3.1 and, consequently, to the number of points visited in the spheres of radius d and dimensions $k = 1, 2, \dots, m$. Hence the expected complexity is proportional to the number of points in such spheres that the algorithm visits on average. Thus the expected complexity of SD algorithm is given by

$$C(m, \sigma^2) = \sum_{k=1}^m \underbrace{(\text{expected \# of points in } k\text{-sphere of radius } d)}_{\triangleq E_p(k, d^2)} \times \underbrace{(\text{flops/point})}_{\triangleq f_p(k)}. \quad (\text{A.2})$$

The coefficient $f_p(k) = 2k + 17$ is the number of elementary operations

(additions, subtractions, and multiplications) that the Fincke-Pohst algorithm performs per each visited point in dimension k .

Assume \mathbf{s}_t is the transmitted vector, \mathbf{s}_a is an arbitrary lattice points, the probability that the k -dimensional lattice point \mathbf{s}_a^k lies inside the hypersphere \mathcal{D} around $\mathbf{y} = \mathbf{H}\mathbf{s}_t + \mathbf{n}$ with radius d can be expressed as the incomplete gamma function

$$\gamma\left(\frac{d^2}{2(\sigma^2 + q)}, \frac{n - m + k}{2}\right) = \int_0^{\frac{d^2}{2(\sigma^2 + q)}} \frac{\lambda^{\frac{n-m+k}{2}-1}}{\Gamma\left(\frac{n-m+k}{2}\right)} e^{-\lambda} d\lambda, \quad (\text{A.3})$$

where $q = \|\mathbf{s}_a - \mathbf{s}_t\|^2$.

In communication applications, the expected number of points in k -dimensional hypersphere depends on the modulation we use. Therefore the expected complexity $C(m, d^2, \varepsilon)$ of SD algorithm to find the optimum solution is

1. for a 2-PAM constellation is

$$\sum_{i=1}^{\infty} (1 - \varepsilon) \varepsilon^{i-1} \sum_{k=1}^m f_p(k) \sum_{q=0}^k \binom{k}{q} \gamma\left(\frac{d_i^2}{2(\sigma^2 + q)}, \frac{n - m + k}{2}\right), \quad (\text{A.4})$$

where $\binom{k}{q} = \frac{k!}{q!(k-q)!}$ is the number of k -dimensional lattice points with

$q = \|\mathbf{s}_a - \mathbf{s}_t\|^2$, and d_i is the radius used for i -th search. For QPSK modulation, it can be treated as two dimensional 2-PAM constellation and modify $n = 2N_R$, $m = 2N_T$.

2. for a 4-PAM constellation is

$$\sum_{i=1}^{\infty} (1 - \varepsilon) \varepsilon^{i-1} \sum_{k=1}^m f_p(k) \sum_q \frac{1}{2^k} \sum_{l=0}^k \binom{k}{l} g_{kl}(q) \gamma\left(\frac{d_i^2}{2(\sigma^2 + q)}, \frac{n - m + k}{2}\right), \quad (\text{A.5})$$

where $g_{kl}(q)$ is the coefficient of x^q in the polynomial

$$(1 + x + x^4 + x^9)^l (1 + 2x + x^4)^{k-l},$$

and $\frac{1}{2^k} \sum_{l=0}^k \binom{k}{l} g_{kl}(q)$ is the number of k -dimensional lattice points with

$q = \|\mathbf{s}_a - \mathbf{s}_t\|^2$. And 16-QAM modulation can also be treated as two dimensional 4-PAM constellation from.

3. for a 8-PAM constellation is

$$\sum_{i=1}^{\infty} (1 - \varepsilon) \varepsilon^{i-1} \sum_{k=1}^m f_p(k) \sum_q \frac{1}{4^k} \sum_{j_1+j_2+j_3+j_4=k} g_{kj_1j_2j_3j_4}(q) \gamma \left(\frac{d_i^2}{2(\sigma^2 + q)}, \frac{n-m+k}{2} \right), \quad (\text{A.6})$$

where $g_{kj_1j_2j_3j_4}(q)$ is the coefficient of x^q in the polynomial

$$\binom{k}{j_1, j_2, j_3, j_4} \phi_1^{j_1}(x) \phi_2^{j_2}(x) \phi_3^{j_3}(x) \phi_4^{j_4}(x),$$

and

$$\binom{k}{j_1, j_2, j_3, j_4} = \frac{k!}{j_1! j_2! j_3! j_4!},$$

$$\phi_1^{j_1}(x) = 1 + x + x^4 + x^9 + x^{16} + x^{25} + x^{36} + x^{49},$$

$$\phi_2^{j_2}(x) = 1 + 2x + x^4 + x^9 + x^{16} + x^{25} + x^{36},$$

$$\phi_3^{j_3}(x) = 1 + 2x + 2x^4 + x^9 + x^{16} + x^{25},$$

$$\phi_4^{j_4}(x) = 1 + 2x + 2x^4 + 2x^9 + x^{16}.$$

And 64-QAM modulation can also be treated as two dimensional 8-PAM constellation from. Similar expressions can be obtained for 16-PAM, etc., constellations.

When the Gram-Schmidt process is used to compute the QR factorization $\mathbf{H} = \mathbf{QR}$, roundoff error can build up as the vectors $(\mathbf{Q})_i$ are calculated one by one on a computer. For large i, j , and $i \neq j$, the scalar products $(\mathbf{Q})_i^H (\mathbf{Q})_j$ may not be sufficiently close to zero. Interestingly, a rearrangement of the calculation, known as modified Gram-Schmidt (MGS), yields a much sounder computational procedure[13]. If orthonormality is critical, then MGS should be used to compute orthonormal bases only when the vectors to be orthogonalized are fairly independent, even though the computational complexity of MGS requires about twice as much arithmetic.

Figure 6.1 shows the flowchart of SD algorithm, m is the number of transmit antennas ($m = N_T$). In this figure, we can make a roughly estimation of the computation complexity of SD algorithm. The complexity of a tree search in SD algorithm is $2(N_T+3)$ flops, and the complexity of MGS is about $2N_R N_T^2$ flops. When $N_T = N_R = 4$, 64-QAM modulation, total number of source nodes of search trees is $64^3+64^2+64 = 266304$. If we use the radius setting method in this paper and assume $\frac{E_b}{N_0} = 16\text{dB}$, the expected number of source nodes of search trees is about 70, and the probability of the number of source nodes of search trees that less than 200 is about 95%. Therefore we can use 200 as a terminate condition of the number of source nodes of search trees.

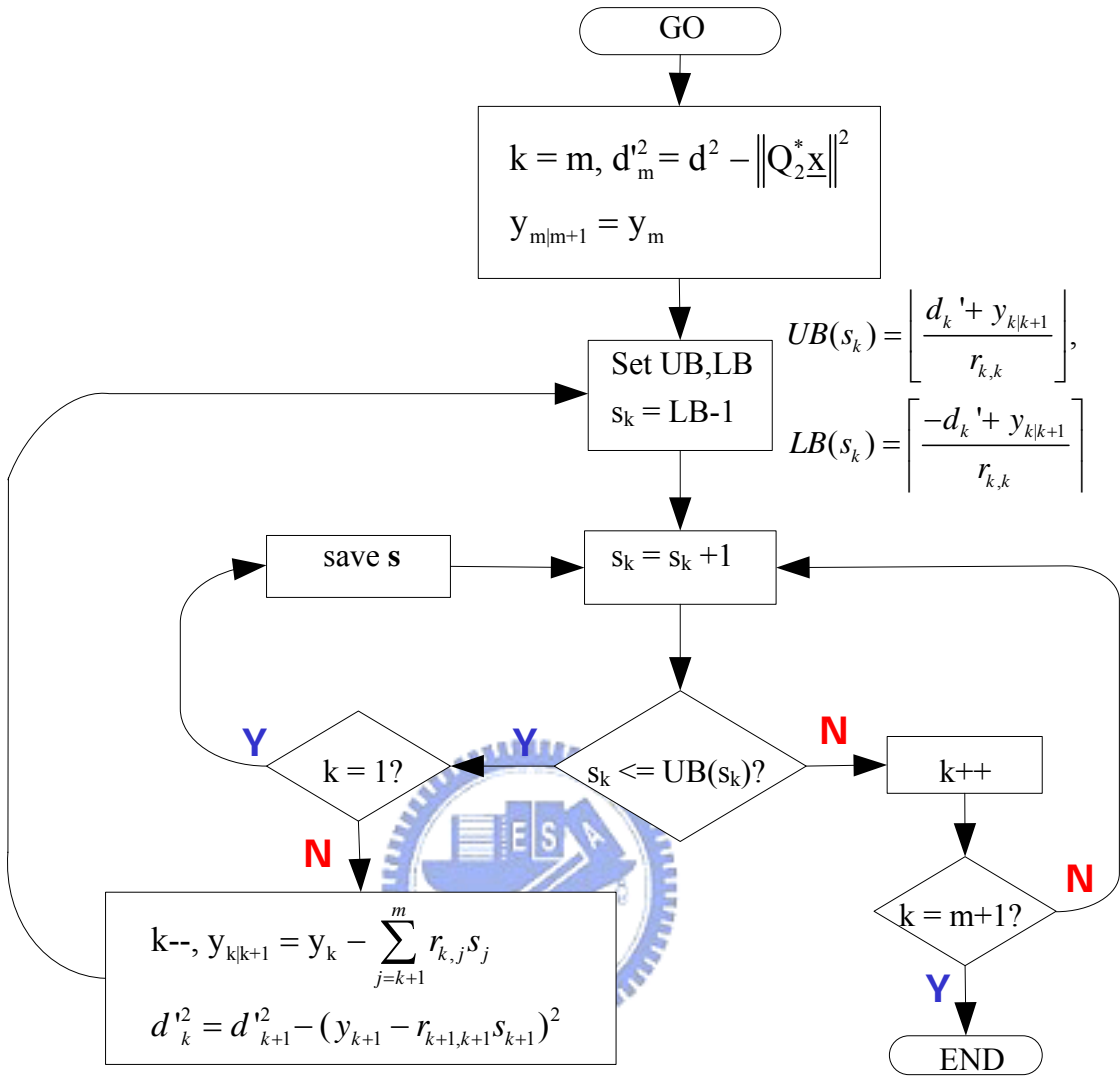


Figure 6.1 The flowchart of decoding algorithm

Assume $N_T = N_R = 4$, 64-QAM modulation, and $\frac{E_b}{N_0} = 16\text{dB}$, a roughly estimation of the complexity of SD algorithm for 802.11n standard in high data rate(40MHz) mode is as follows

$$108(2 \times 4 \times 4^2 + 2 \times (4 + 3) \times 200) / (3.6 \times 10^{-6}) = 8.784 \times 10^{10} \text{ flops}$$

Appendix

Proof of probability density function(pdf) of $\min_i \|(\mathbf{H})_i\|$, where \mathbf{H} is a m -by- n complex Gaussian matrix :

The i -th column norm of matrix \mathbf{H} can be expressed as :

$$\|(\mathbf{H})_i\| = \sqrt{\sum_{j=1}^N |h_{ji}|^2}, i = 1, \dots, M,$$

and

$$|h_{ji}|^2 = \Re\{h_{ji}\}^2 + \Im\{h_{ji}\}^2.$$

Assume $\Re\{h_{ji}\}$ and $\Im\{h_{ji}\}$ are both $N(0, \sigma^2)$ distribution, where $\sigma^2 = \frac{1}{2}$. Then the distribution of $|h_{ji}|^2$ is $E(\lambda)$ and the distribution of $\|(\mathbf{H})_i\|^2$ is $\Gamma(N, \frac{1}{\lambda})$, where $\lambda = \frac{1}{2\sigma^2}$.

For convenience, let

$$\text{r.v. } Y_i = \|(\mathbf{H})_i\|, i = 1, \dots, M,$$

and

$$\text{r.v. } Z = \min_i (Y_i).$$

The pdf of random variables Y_i can be derived easily as

$$f_{Y_i}(y) = \frac{2\lambda^N y^{2N-1} e^{-\lambda y^2}}{\Gamma(N)} u(y), i = 1, \dots, M.$$

The cumulative distribution function (CDF) of random variable Z is derived as follow

$$F_Z(z) = \Pr[\min_i(Y_i) \leq z]$$

$$= 1 - \beta^M e^{-\lambda M z^2} \left[\gamma z^{2N-2} + 2(N-1)\gamma^2 z^{2N-4} + \dots + 2^{N-1} \prod_{k=1}^{N-1} k \gamma^N \right]^M$$

where $\beta = \frac{2\lambda^N}{(N-1)!}$, $\gamma = \frac{1}{2\lambda}$, and $z \geq 0$.

By differentiating the CDF of random variable Z we obtain the pdf

$$f_Z(z) = -M\beta^M e^{-\lambda M z^2} \left[\gamma z^{2N-2} + 2\gamma^2(N-1)z^{2N-4} + \dots + 2^{N-1}\gamma^N \prod_{k=1}^{N-1} k \right]^{M-1} \times$$

$$\left\{ 2\gamma z^{2N-2} [z^{-1}(N-1) - \lambda z] + 2^2 \gamma^2 (N-1) z^{2N-4} [z^{-1}(N-2) - \lambda z] + \dots + 2^N \gamma^N \prod_{k=1}^{N-1} k (-\lambda z) \right\}$$

$$= -M\beta^M e^{-\lambda M z^2} [(N-1)!]^M \left[\sum_{i=1}^N \frac{2^{i-1} \gamma^i z^{2(N-i)}}{(N-1)!} \right]^{M-1} \left\{ \sum_{i=1}^N \frac{2^i \gamma^i z^{2(N-i)} [(N-i)z^{-1} - \lambda z]}{(N-1)!} \right\},$$

and $z \geq 0$.



Reference

- [1] B. Hassibi and H. Vikalo, "On the Sphere Decoding Algorithm. I. Expected Complexity," *IEEE transactions on signal processing*, vol. 53, no. 8, pp. 2805-2818, Aug. 2005.
- [2] M. O. Damen, H. E. Gamal, and G. Caire, "On Maximum-Likelihood Detection and the Search for the Closest Lattice Point," *IEEE transactions on information theory*, vol. 49, no. 10, pp. 2389-2402, Oct. 2003.
- [3] O. Damen, A. Chkeif, and J.-C. Belfiore, "Lattice Code Decoder for Space-Time Codes," *IEEE communications letters*, vol. 4, no. 5, pp. 161-163, May 2000.
- [4] L. M. Davis, "Scaled and Decoupled Cholesky and QR Decompositions with Application to Spherical MIMO Detection," *Proc. IEEE WCNC*, pp. 326-331, Mar. 2003.
- [5] P. Wolniansky, G. Foschini, G. Golden, and R. Valenzuela, "V-BLAST: An Architecture for Realizing Very High Data Rates over the Rich-Scattering Wireless Channel," *Proc. ISSSE*, pp. 295-300, Sept. 1998.
- [6] U. Fincke and M. Pohst, "Improved Methods for Calculating Vectors of Short Length in Lattice, Including a Complexity Analysis," in *Mathematics of Computation*, Apr. 1985, vol. 44, no. 170, pp. 463-471.
- [7] J. Jalden and B. Ottersten, "On the Complexity of Sphere Decoding in Digital Communications," *IEEE transactions on signal processing*, vol. 53, no. 4, pp. 1474-1484, Apr. 2005.

- [8] B. Hassibi and H. Vikalo, "On the Sphere Decoding Algorithm. II. Generalizations, Second-Order Statistics, and Applications to Communications," *IEEE transactions on signal processing*, vol. 53, no. 8, pp. 2819–2834, Aug. 2005.
- [9] A. Paulraj, R. Nabar, and D. Gore, *Introduction to Space-Time Wireless Communications*. Cambridge Univ. Press, 2003.
- [10] M. O. Damen, K. Abed-Meraim, and J.-C. Belfiore, "Generalized Sphere Decoder for Asymmetrical Space-Time Communication Architecture," *Electronics letters*, vol. 36, no. 2, pp. 166–167, Jan. 2000.
- [11] P. Dayal and M. K. Varanasi, "A Fast Generalized Sphere Decoder for Optimum Decoding of Under-Determined MIMO Systems," in *Proc. of 41st Annual Allerton Conf. on Comm. Control, and Comput.*, Oct. 2003.
- [12] T. Cui and C. Tellambura, "An Efficient Generalized Sphere Decoder for Rank-Deficient MIMO Systems," *IEEE communications letters*, vol. 9, no. 5, pp. 423–425, May 2005.
- [13] G. H. Golub and C. F. V. Loan, *Matrix Computations*, 2nd ed. John Hopkins Univ. Press, 1989.
- [14] D. Tse and P. Viswanath, *Fundamentals of Wireless Communication*. Cambridge Univ. Press, Sept. 2004.
- [15] D. Pham, K. R. Pattipati, P. K. Willett, and J. Luo, "An Improved Complex Sphere Decoder for V-BLAST Aystem," *IEEE signal processing letters*, vol. 11, no. 9, pp. 748–751, Sept. 2004.